A common thread in the evolution of the configurations of supercritical CO_2 power systems for waste heat recovery

Gianluca Carraro [a], Piero Danieli [a], Andrea Lazzaretto [a,], Tazio Boatto [a]*

[a] = *Dept. of Industrial Engineering, University of Padova, Via Venezia 1, 35131 Padova, Italy.*
gianluca.carraro@unipd.it, piero.danieli@unipd.it, tazio.boatto@unipd.it

**= corresponding author, andrea.lazzaretto@unipd.it*

Abstract

Several configurations of supercritical CO_2 (sCO_2) power systems have been recently proposed as promising solutions for power generation from medium-temperature heat sources (300 °C – 700 °C). The paper exploits the potential of a methodology called "HEATSEP" to review and analyse critically the conceptual development of these configurations, when applied to waste heat recovery. The goal is to find a common thread in the evolution of all sCO_2 configurations proposed in the literature for waste heat recovery, and search for new, more performing ones. As required by the HEATSEP method, the study is performed by separating each configuration in two parts: a part, named "basic configuration", including all components that are necessary to realize the "basic concept" on which the system is based on, and the remaining part associated with the internal heat transfers and the heat exchanger network that realize them. The paper shows that all the "basic configurations" of sCO_2 power systems presented in the literature are created by including one or more splitters after the compression process, and then re-joining the separate streams in different manners. All these configurations are included in a general evolution tree, showing how they have evolved logically and why. Starting from the most performing configurations in the literature, the HEATSEP method enables to identify possible power output improvements by exploiting heat transfers not yet considered. Results show that the possible power gains are very small (4 kW out of 480 kW) demonstrating that the literature configurations have negligible margins for improvements.

Keywords

Waste heat recovery, Supercritical CO_2 power system, System configurations, HEATSEP method, Design optimization, Performance comparison

Nomenclature

Symbols		p	pump
p	pressure, bar	tot	total
T	temperature, °C	hs	heat source
$\dot{m}$	mass flow rate, kg/s	co2	carbon dioxide
$\dot{Q}$	thermal power, kW	is	isentropic
h	enthalpy, kJ/kg	w	water
P	power, kW	t	turbine
Greek symbols		**Abbreviations**	
η	efficiency	sCO_2	supercritical CO_2
φ	heat recovery effectiveness	HEATSEP	heat separation
Δ	difference	WHR	waste heat recovery
Subscripts		LTT	low temperature turbine
el	electrical	HTT	high temperature turbine
lim	limit	TIT	turbine inlet temperature
mec	net mechanical	COOL	cooler
c	compressor	HE	heater
in	inlet	REG	regenerator
out	outlet	SS_DH	single split double heating
rec	recovery	SS_DE	single split double expansion
th	thermal	DS_DH	double split double heating
max	maximum	DS_DE	double split double expansion
av	available		
cool	cooler		
min	minimum		
pp	pinch point		

1. Introduction

The main strategy of the European Union to reduce greenhouse gas emissions is based on the promotion of renewable energy penetration and the increase of energy efficiency. In 2018, new EU directives set targets for 2030 of a 32 % share for renewable energy and at least a 32.5 % improvement in energy efficiency (compared to the values of 1990) [1]. The conversion of waste heat to electric power is one of the most viable options to achieve the energy-efficiency target by improving the efficiency of existing industrial plants. Waste heat sources in-between 300 °C and 700 °C pose the challenge to choose a bottoming power system that could be affordable, compact and efficient at the same time. In this context, conventional steam Rankine cycles are economically feasible only for large sizes (>50 MW) due to the high specific volume of steam, while Organic Rankine Cycle (ORC) systems may face problems associated with the working fluids characteristics (such as high cost and thermal degradation [2]). Recently, the supercritical carbon dioxide (sCO_2) Brayton cycle has been proposed as a third promising solution that could potentially overcome the issues of the other two power systems [3-5]. The main characteristics of sCO_2 systems are summarized in the following:

- The thermodynamic cycle operates in the supercritical region because the critical temperature of the CO_2 is close to the ambient one. Due to this property of CO_2, the heat rejection phase of the supercritical cycle can easily lead the fluid conditions at the compressor inlet close to the critical point. In these conditions, the high density of the CO_2 vapor [6] (close to that of the liquid phase) allows to strongly reduce the compression work (which is similar to that of a pump) and, in turn, to increase the cycle efficiency.
- The high density in the vapor phase reduces the dimensions and costs of the components.
- CO_2 is a natural, non-toxic and non-flammable fluid.

The sCO_2 power cycle was originally conceived as a closed cycle to replace the Steam Rankine cycle in stand-alone applications such as nuclear [7, 8] and concentrated solar thermal power [9]. In these applications, the cooling of the heat source is typically limited to temperature values that guarantee good and stable operation of the thermal power generator (either nuclear reactor or solar receiver) [10]. Thus, for given features of the heat source, the aim of the research about these power plants is *the maximization of the thermal efficiency of the sCO_2 system*. The search for the highest thermal efficiency η_{th} (defined as the ratio between the power generated by the expander and the amount of heat absorbed in the heater) implies the increase of the mean temperature at which the heat is supplied to the system. To maximize this temperature, as much heat as possible should be internally regenerated. The layout of the recompression cycle has been specifically conceived with the purpose of maximizing the thermal efficiency by optimizing the internal regeneration of the heat [11]. In this cycle, a fraction of the CO_2 mass flow rate does not enter the cooler but is compressed and directly sent to the high temperature recuperator, after which it absorbs heat from the heat source and subsequently is expanded in the turbine.

Another appealing application of CO_2 systems consists in using the products of the oxy-fuel combustion of methane to run a CO_2-based power cycle. In fact, the oxy-combustion of methane takes methane, oxygen and CO_2 as inputs and gives CO_2 as the main output (in addition to water, which, however, accounts for a smaller quantity). This process was also proposed with the addition of water as moderator in the combustion chamber, so that the resulting power cycle is a water-CO_2 cycle of very high efficiency operating in both open ([12]) and closed configuration ([13]). In this context, Costamagna [14] smartly revisited the idea of closed CO_2 power cycle with oxy-combustion to give an answer to the mismatch between the power generation from intermittent renewable sources and the user demand. She suggested the "three-pipeline gas grid (3PGG)" concept, which considers the addition of a twin distribution grid conveying oxygen and CO_2 to the existing gas distribution network. Oxygen (O_2) is generated by an electrolyser fed by photovoltaic electricity and sent to the O_2 grid. CO_2 is generated by the oxy combustion of methane of the power cycle, where methane derives from methanation of H_2 (also obtained by the electrolyser) using the CO_2 itself that is conveyed in the CO_2 pipeline. Thus, the CO_2 pipeline closes the CO_2 cycle and the whole process allows transferring carbon from the methane to the carbon dioxide pipeline and vice versa, without ever releasing it into the atmosphere.

In addition to the above-mentioned applications, CO_2 systems have been studied also as bottoming cycles of a topping process. This category includes waste heat recovery applications, in which, unlike stand-alone ones, the search for performing layouts should pursue not only the goal of maximizing η_{th} but also the additional goal of exploiting as much as possible the heat available from the heat source. In this context, two more performance metrics gain importance, namely the "heat recovery effectiveness φ" (defined as the ratio between the heat supplied to the the system and the overall heat available from the heat source) and the "total heat recovery efficiency η_{tot}", which is the ratio between the power output and the overall heat available from the heat source or, in other words, the ratio between the thermal efficiency and the heat recovery effectiveness [15].

The potential of the recompression cycle layout (originally designed for stand-alone applications) was also investigated for waste heat recovery (WHR) applications [16]. Mohammadi et al. [17] compared the thermodynamic and economic performance of six different power systems including four sCO_2 power cycles (sCO_2 Rankine cycle, simple regenerative sCO_2 cycle, recompression sCO_2 and partial cooling sCO_2 cycle) and two ORCs (simple and regenerative ORC) to identify the most promising option in the exploitation of the waste heat from an upper Brayton cycle. With a heat source temperature of 394 °C, the ORC system with Toluene achieved the highest power output (2506 kW) and the lowest Levelized Cost Of Electricity (LCOE, 21.68 \$/MWh). Among the sCO_2 systems, the partial-cooling and the simple regenerative cycles attained higher power output (1580 kW and 1489 kW, respectively) than the recompression one (1280 kW). It is worth noticing that the latter system showed the lowest power output and the highest thermal efficiency (32.0 %) compared to all the other heat recovery systems. Moroz et al. [18] pointed out that, in the whole range of TITs going from 300 °C to 500 °C, the heat recovery effectiveness of the simple regenerative layout is 2 % higher than that of recompression and pre-compression ones. This characteristic is the main reason that let the authors conclude that, among the three, the simple regenerative layout is the most suitable one for waste heat recovery.

It is quite evident that, in waste heat recovery applications, stand-alone sCO_2 layouts, such as recompression, partial cooling and precompression ([19]), lose their advantage on the simple regenerative layout. The main reason is their inability to cool down the heat source [20], preventing the system from achieving high power output. One of the most effective solutions to increase both φ and η_{tot} is to put in series two separate sCO_2 stand-alone layouts in a cascaded system [21]. In spite of the better exploitation of the heat source and the consequent power output gain [18], these systems pay for greater complexity and costs [22], devising the need to conceive innovative layouts for waste heat recovery applications.

In the last years, a lot of works proposed different configurations for waste heat recovery applications and systematically compared them from a thermodynamic point of view [23]. For completeness, Table A.1 in Appendix A gives an overview of the main sCO_2 system configurations for waste heat recovery available in the literature and reviewed in this Section. For each configuration, Table A.1 specifies its name (as from the literature), shows a schematic of the layout, and reports the key performance data taken from some reference works in the literature.

The comprehensive review of Crespi et al. [24] highlighted that the main ingredients of bottoming sCO_2 cycles (i.e., WHR layouts) are "split-flow before heating" (SFH) and "split-flow before heating and expansion" (SFHE). One of the most simple and promising WHR configurations that can be generated by splitting the CO_2 mass flow rate, is the partial heating cycle [25, 26] (configuration c) in Table A.1). Na et al. [27] explored its potential in comparison with the simple regenerative one. The contribution of the second heater (named "preheater") to the increase of power production was evaluated by allocating a different share (ψ) of the total UA product of the system among the heat exchangers. This means that, if ψ of the second heater is equal to zero, the second heater does not work and the partial heating layout degenerates into the simple regenerative one. Being UA a measure of the heat exchangers size, the perspective was that of obtaining the partial heating layout while keeping the system compact. An increase of ψ of the second heater from 0 % to 13 % entails an increase of the power output from 7.8 MW to 8.6 MW.

If the two mass flow rates generated by the splitter are not re-joined in the high-pressure part of the cycle (as in the partial heating layout), but in the low-pressure part, the sCO_2 cycle includes a double expansion. The inclusion of a second turbine aims at increasing the maximum TIT of the cycle [28] due to the presence of two high-pressure sCO_2 streams that enable a higher flexibility in the process of cooling down the heat source. Particularly, three layouts with a splitter and the double expansion drew the attention of the researchers [23, 29]. The first layout is the "single flow split with dual expansion" layout (as called in [29], configuration d) in Table A.1), in which, one of the two CO_2 streams generated by the splitter after the compressor is heated by the waste source before entering the high temperature turbine, while the other CO_2 stream is heated in a low and high temperature regenerators and expanded in the low temperature turbine. The second layout is the "dual recuperated" layout (as called in [29, 30], configuration e) in Table A.1), in which, one of the two streams generated by the splitter after the compressor goes through the high temperature recuperator and enters the low temperature turbine, whereas the other is heated by the low temperature recuperator and by the heater before going across the high temperature turbine. Finally, the third layout is the "dual heated cascade" layout (as called in [31], configuration f) in Table A.1), in which, the stream of the high temperature turbine is heated (before entering the turbine itself) first by the two regenerators and secondly by the heater, whereas the stream of the low temperature turbine absorbs heat through a second heater that recovers the residual heat of the waste source. Wright et al. [30] compared η_{th}, φ, η_{tot} and costs of the single flow split with dual expansion, dual recuperated and partial heating layouts. With the heat source at 538 °C, the simple regenerative layout achieved a η_{tot} of 17.3 %, which was at least 3 % lower than that of the other layouts (in the range from 20.3 % to 21.2 %). About costs, a key finding was that, leaving out the simple regenerative layout, the dual recuperated one showed the lowest capital investment costs (15729 M$). The thermodynamic performance of the same layouts was evaluated also by Manente and Costa [32], who optimized the cycles in the exploitation of waste heat at 600 °C. The authors made the effort of decomposing the structure of the cycles into elementary Brayton cycles to understand the contribution of each of them to the overall performance [33]. Results highlighted that the layouts with two turbines were able to reach TITs that were substantially higher (more than 150 °C) than those of the single-turbine layouts. Moreover, the dual recuperated layout achieved the highest thermal efficiency (28.4 %), whereas the single flow split with dual expansion layout showed the highest total heat recovery efficiency (22.3 %). Marchionni et al. [34] assessed eight different sCO_2 system configurations from a techno-economic point of view. The layouts could be subdivided into two main groups: conventional layouts (among which simple regenerative and recompression cycles) and innovative layouts (including the partial heating and dual expansion cycles). The innovative layouts demonstrated a higher capability of cooling down the heat source (exhaust gas at 650 °C) and, compared to the traditional ones, showed an increase of power output that ranged from 9 kW to 79 kW. In particular, the partial heating layout and the dual heated cascade cycle (called “pre-heating split-expansion”) achieved the highest power output (171 kW and 165 kW, respectively). However, the authors highlighted that, in spite of the poorest performance, the simple regenerative layout is the most cost effective one due to the lowest complexity (specific cost of 770 $/kWe and payback period of 1.86 years).

A further increase of the complexity of sCO_2 layouts (with respect to the three layouts with double expansion described above) involves the addition of a junction-splitter couple after the first splitter in the high-pressure part (configuration g) in Table A.1). This layout (called “dual flow split with dual expansion” in [29]) was first proposed by Kimzey [35] in comparison with the single flow split with dual expansion and the dual heated cascade layouts. These systems were evaluated as bottoming cycles of two different gas turbines having as benchmarks steam bottoming cycles of 195 MW and 14 MW, respectively. The dual flow split with dual expansion system was the best performing sCO_2 system, with a power output of 15.2 MW (from 0.4 MW to 1.8 MW higher than the other cycles) in the case of the lower size gas turbine and a power output of 169 MW (from 8 MW to 36 MW higher than the other cycles) in the other case. Manente and Fortuna [29] confirmed the high performance of the dual flow split with dual expansion layout, which achieved a total heat recovery efficiency from 5.8 % to 9.5 % higher than that of the conventional layouts (i.e., the simple regenerative and the recompression cycles), depending on the temperature of the waste heat source (400 °C - 800 °C). Thanganadar et al. [36] considered the problem of optimizing a combined power cycle (CPC) based on a gas turbine and a sCO_2 system as a whole, instead of finding the optimal design of only the sCO_2 system for given exhaust conditions. They analysed four different sCO_2 system layouts taken from the literature and proposed a novel configuration. From the first simplest layout (called “Cascade 1”) to the last most complex one (called “Cascade 5”), the addition of multiple heating and/or expansion processes aims at minimizing the heat transfer irreversibilities in heaters and regenerators (i.e., searching for the perfect thermal match). The first three configurations, that is, “Cascade 1, 2 and 3” cycles are the single flow split with dual expansion, the dual-heated cascade and the dual flow split with dual expansion cycles, respectively. The “Cascade 4” cycle was derived by the “dual rail” cycle proposed by Echogen in [37] and the “Cascade 5” cycle is a novel cycle with four heating stages, three turbines and three regenerators. For a gas turbine TIT of 1316 °C, the maximum net efficiency of the CPC system (defined as the net power produced by the gas turbine and the sCO_2 system divided by the combustion energy) increased from 56.6 % to 59.7 % going from Cascade 1 to 5 cycles. The increase of the efficiency does not compensate the increase of the investment cost, so that Cascade cycles 4 and 5 are not economically attractive. The best compromise is Cascade 3 cycle (i.e., the dual flow split with dual expansion), which showed the lowest cost of electricity for all studied gas turbine TIT. Kim M.S. et al. [31] carried out a thermodynamic comparison between nine sCO_2 power cycle layouts, including some conventional layouts (simple regenerative, recompression and pre-compression), the partial heating layout, the three layouts in [35] and three new ones proposed by the authors. All layouts were evaluated as bottoming cycles of a 5.0 MW gas turbine, which provided exhaust gases at the temperature of 520 °C. Results highlighted that the new layouts conceived by the authors were not able to produce more power than the partial heating layout. On the other hand, the layouts in [35] showed promising performance and two out of three outperformed the partial heating in terms of power output (3.02 MW and 3.23 MW of the dual heated cascade and dual flow split with dual expansion layouts, respectively, versus 2.75 MW of the partial heating layout).

1.1. Aim and novelty of the study

The majority of works proposing and evaluating different sCO_2 system configurations for waste heat recovery deal with the thermodynamic performances and technological aspects of specific configurations whereas only few of them put the accent on the principles that guide the conception of the different layouts (see, e.g. [32]). In this paper, a new perspective is drawn to enable a critical review of these works within a clear logic of evolution of the sCO_2 cycle configurations.

The goal is twofold:

1. Identifying a general criterion for the construction of the most promising configurations for waste heat recovery. This criterion allows outlining a common thread in the evolution of these configurations, starting from the simplest one to gradually increase the layout complexity. The idea is that of providing a framework that "at a glance" can explain how and why the configurations have been generated.
2. Analysing critically the configurations proposed in the literature, reconsidering their conception starting from the elementary components they are based on, to identify possible directions to conceive new layouts. In particular, the configuration built upon a given cycle architecture is evaluated in two ways: i) considering all its components, as usually done, and ii) with a methodology called "HEATSEP" [38, 39], which separates the construction of the basic architecture (called "basic configuration") from the construction of the internal heat exchangers network. This allows understanding whether new layouts with higher performance can be obtained from that architecture, by means of a complete exploitation of the internal heat transfer interactions.

The main contribution will be that of providing an easy "recipe" and common rules that, on the one side, help understand the basics, potential and limits of existing configurations and, on the other side, identify new possible layouts.

2. Key points in the evolution of high-power-output sCO_2 cycle configurations

The main limitation of operating in the supercritical region is the low pressure ratio. Pressure ratios are of the order of 2-3 to limit the maximum pressure of the cycle (to the values allowed by the existing machines [40, 41], e.g., 251 bar in [42]), given that the suction side of the compression is close to the critical pressure (73,9 bar). This in turn implies the need of regeneration to achieve good cycle efficiency. The simplest regenerative configuration consists of compressor, heater, turbine, regenerator (which exploits the high enthalpy content of the gas exiting the turbine to preheat the stream at the outlet of the compressor), and cooler.

The evolution of this configuration must search for the optimum compromise between the following specific requirements to achieve high power output:

1) Good thermal match in the regenerator;
2) Complete cooling of the heat source in the heater;
3) Good thermal match in the heater;
4) Best compromise between mass flow rate and TIT of the turbine (both should be maximized).

The key point to reach this compromise is the *inclusion of a splitter at compressor exit*, to make the heat recovery in the regenerator independent of the heat recovery in the heater. In fact, the splitter allows the mass flow rates sent to the two heat exchangers to be properly balanced to find, on one side, the best thermal match in the regenerator and, on the other side, to achieve the maximum exploitment of the energy content of the heat source. All the heat recovery system configurations proposed in the literature that are able to supply high power output *include one or more splitters after the compressor* (Fig. 1). The two different mass flow rates generated by each splitter are *consequently re-joined in one or more junctions*, since the sCO_2 systems under consideration are closed cycles.

These configurations differ basically

i) for the different locations of the junctions where the mass flow rates generated by the splitters re-join,

ii) for the components included between splitters and junctions, and

iii) for the different values of the basic design parameters (in particular, of the mass flow rates and TIT of the turbine).

To get a clear picture of the evolution of the configurations according to this criterion, it is worth looking at the cycle architectures without considering the heat exchanger networks that realizes the internal heat transfer, as the HEATSEP method suggests (see [39, 43]). Thus, only "basic" components, namely compressor, splitter, junction and turbine are included. The internal heat exchangers are initially excluded to "cut the thermal links" (thermal cut zones in Fig. 1) between the basic components in order to let the temperatures between them free to vary, and to find subsequently their best possible values by means of an optimization procedure (Section 4). These values allow calculating the optimal hot-and-cold internal thermal streams that lead to the construction of the optimal hot-and-cold composite curves of the "basic configuration" under consideration (Section 5). In a subsequent step, the optimal internal heat exchangers network can be built on the basis of these thermal streams [44].

The evolution logic of the "basic configurations" of the sCO_2 systems is shown in the tree diagram of Fig. 1, called here "Evolution Tree". Starting from the most basic architecture, i.e., the "simple" one, only one compressor and one turbine are included. The inclusion of a splitter at compressor exit (split 1) generates other two possible architectures that differ for the different locations of the junctions. In fact, the split-flowrates can re-join either in the "heating zone" or in the "expansion zone", thereby obtaining the Single Split Double Heating (SS_DH) or the Single Split Double Expansion (SS_DE) layouts, respectively.

The screening of the works in the literature points out more advanced configurations that are based on a second splitter (split 2) of mass flow rates after the first junction. Hence, the inclusion of a second splitter is also considered in drawing a general line of evolution. The splitting can therefore occur either after the junction in the heating zone (evolving the SS_DH architecture) or after the junction in the expansion zone (evolving the SS_DE architecture). However, in the latter case, the generation of additional streams in the low pressure part of the cycle does not help satisfy the requirements specified in Section 1.2, as the red cross highlights in Fig. 1. In that part of the cycle, a beneficial independency between regeneration and cooling of the heat source can be found only if one of the two mass flow rates is compressed again. This option is accomplished, for example, in those configurations, like the recompression cycle, which include a splitter before the compressor [45].

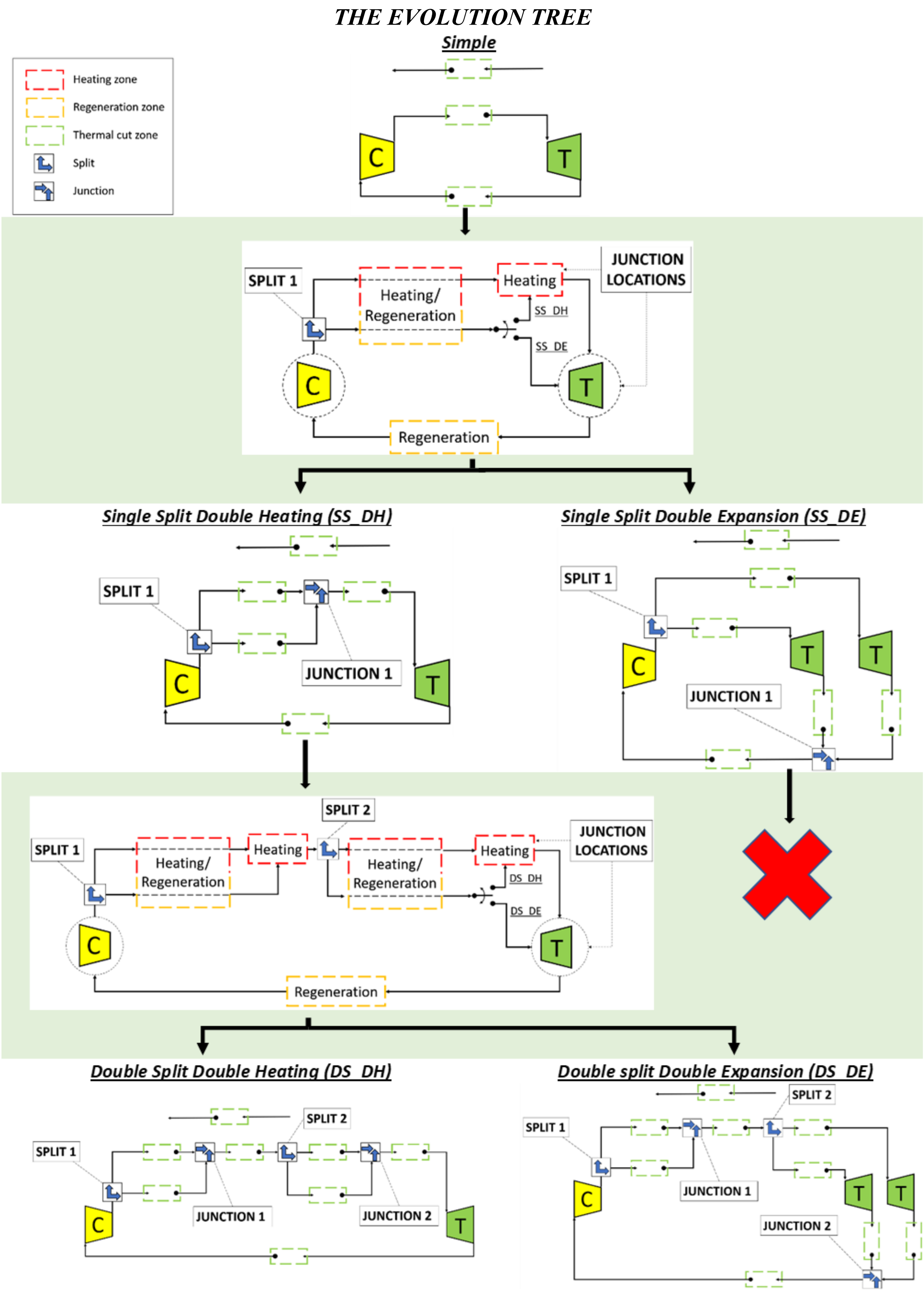

Fig. 1. Evolution tree of the sCO_2 power system configurations for WHR applications

They tipically result in high efficiency but are not intrinsically able to exploit a high percentage of the energy content of the heat source. For this reason, they are neglected here (examples of these configurations are shown in [46]). By contrast, the SS_DH configuration with a second split placed in the heating zone, has the potential to evolve into two promising architectures. If the second junction (junction 2) is placed in the heating zone like the first one, the Double Split Double Heating (DS_DH) layout is generated. If, in turn, the mass flow rates re-join in the expansion zone, the Double Split Double Expansion (DS_DE) layout is obtained.

It is worth reminding that, as mentioned in Section 1.1, this evolution structure of the sCO_2 configurations for WHR systems is studied in the following in two different ways:

1) considering all components belonging to each architecture, as usually done in the literature of energy systems modelling, and

2) using the HEATSEP approach, i.e., considering the “basic configuration”, while leaving the construction of the heat exchangers network as a separate step to be performed separately (after the optimization of the basic configuration).

3. Inclusion of the configurations proposed in the literature in the evolution tree

In this Section, the different configurations proposed in the literature including the internal heat exchangers networks have been analyzed according to the categories highlighted in the Evolution Tree in Fig. 1. For each category (i.e., for each “basic configuration”), the most performing configuration has been chosen in accordance with the literature, explaining basic concepts, potentialities and limits. Although the names of these configurations may differ in the literature from those used in Section 2, the authors believe that the nomenclature introduced in this study helps analyze step by step all the configurations for WHR, i.e., having single or multiple splitters after the compression.

3.1 Simple Regenerative

The three thermal cuts shown in the SIMPLE basic configuration in Fig. 1 are solved in the literature by means of the simple regenerative layout in Fig. 2. Note that the easiest way to fill out the thermal cuts would have been that of a simple sCO_2 cycle without regenerator. However, it would have certainly led to a less efficient solution [17]. The basic regenerative configuration simply includes a regenerator after the compressor to recover the heat content of the CO_2 after the expansion. A good benchmark for this simple layout is the work of Danieli et al [47], in which the performance of the simple regenerative sCO_2 system is compared with that of a simple air Brayton cycle and an ORC system in the utilization of the flue gas at 470 °C from furnaces for hollow glass production. Results showed that the sCO_2 system could generate the maximum power output (457 kW), which is 47 % and 157 % higher than that of the cyclopentane ORC and air Brayton-Joule cycle systems, respectively. The sCO_2 layout is able to achieve that performance only if the flue gas temperature is increased to 648 °C by means of a preheating system that increases the combustion air temperature of the furnace using the low temperature heat that is not exploited by the sCO_2 cycle. In absence of this preheating system, the simple regenerative sCO_2 system achieved a power output that was 37 kW lower than that of the ORC system. As mentioned in the Introduction, the presence of a regenerator can increase the thermal efficiency of the sCO_2 system but, at the same time, imposes a high temperature of the CO_2 entering the heater that hinders the exploitation of the low temperature heat of the heat source. Table 1 summarizes the main operating parameters of the simple regenerative sCO_2 cycle in the waste heat recovery application addressed in [47].

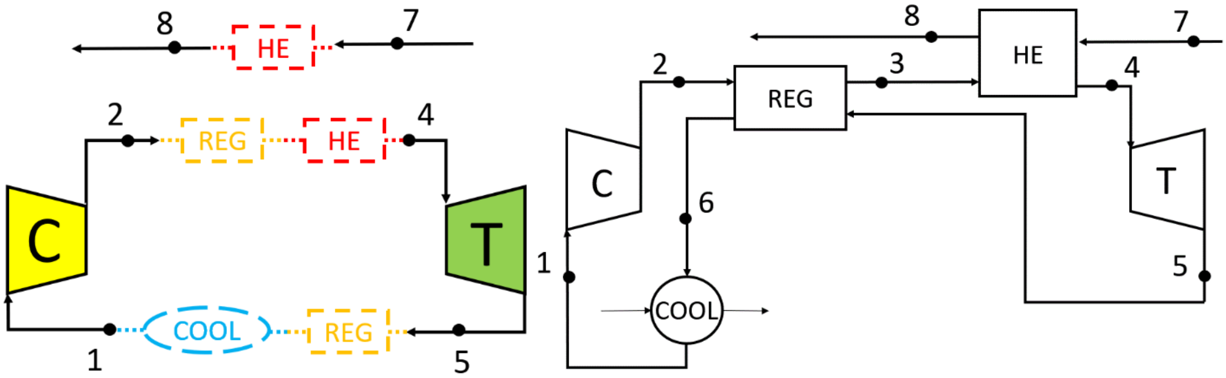

a) b)

Fig. 2. Layout of the SIMPLE configuration: a) integration of the heat exchanger network into the basic configuration of the Evolution Tree and b) the resulting configuration from a) proposed in the literature.

3.2 Single Split Double Heating

The inclusion of a splitter of the mass flow rate after the compressor evolves the SIMPLE architecture by the addition of two more thermal cuts. This architecture is solved in the literature by the addition of a second stage heater (HE-2 in Fig. 3(a)) that yields the single split double heating (SS_DH) configuration in Fig. 3(b). By means of the splitter, a fraction of sCO_2 (stream 2' in Fig. 3(b)) is delivered to a second stage heater (HE-2) and the rest (stream 2'') to the regenerator (REG). This allows to decouple the regenerative process from the cooling of the heat source and to achieve a remarkable improvement of both the regeneration (thanks to an improved thermal match) and the heat recovery effectiveness. The two streams of sCO_2 are then remixed before the first heat exchanger (point 5). Kim Y.M. et al. [26] confirmed the superiority of the SS_DH layout over the SIMPLE one in terms of power output and heat recovery effectiveness. Exploiting exhaust gas at 538 °C, the SS_DH layout achieved a power output of 10640 kW with a heat recovery effectiveness of 89.6 % and a total heat recovery efficiency of 26.0 %. On the other hand, the same performance metrics for the SIMPLE layout showed values of 8129 kW, 69.2 % and 19.9 %, respectively. Based on [26], the working conditions of the SS_DH layout as bottoming cycle of a 25 MWe gas turbine are highlighted in Table 1.

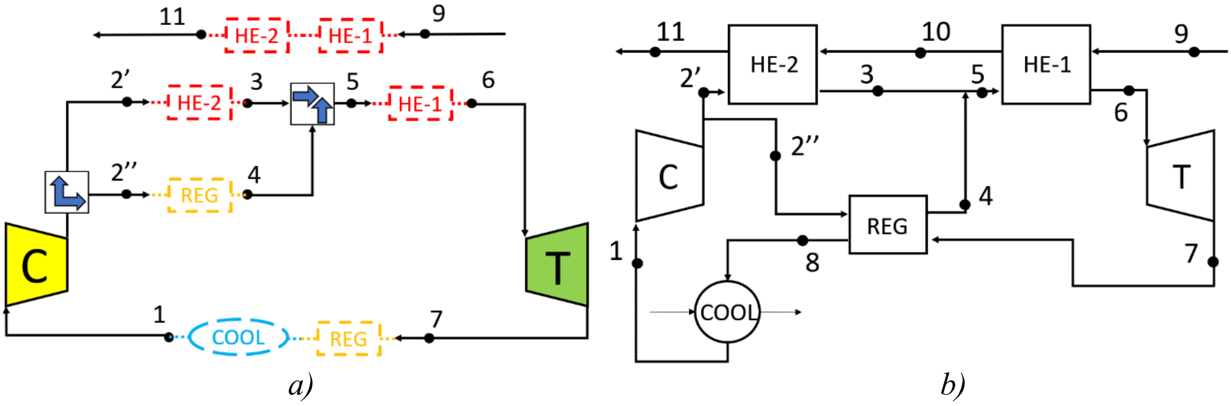

Fig. 3. Layout of the SS_DH configuration: a) integration of the heat exchanger network into the basic configuration of the Evolution Tree and b) the resulting configuration from a) proposed in the literature.

3.3 Single split double expansion

The difficulty of the SS_DH layout to reach TITs close to the heat source temperature [29] is tackled with the addition of a second turbine that leads to the single split double expansion basic configuration (SS_DE in Fig. 1). Starting from this basic architecture, several configurations arose in the literature. The most promising of them have been already mentioned in Section 1, namely the single flow split with dual expansion [32], the dual heated cascade [31] and the dual recuperated [30] layouts. According to the literature, it is not straightforward to identify the best performing layout in terms of power output. In [30], the dual recuperated layout generated more power (8322 kW) with respect to the single flow split with dual expansion layout (8214 kW), but was outperformed by the SS_DH layout (8601 kW). In [31], the dual heated cascade cycle achieved the highest power output (3.02 MW) among the layouts with one splitter and double expansion. It performed better than both the single flow split with dual expansion (2.68 MW) and the SS_DH (2.75 MW) layouts. In [32], the single flow split with dual expansion attained a power output that was 3.1 % higher than that of the SS_DH layout and 15 % higher than that of the dual recuperated layout. In [34], the dual heated cascade achieved the highest power output together with the SS_DH layout and outperformed the single flow split with dual expansion one. The lack of an unquestionable decision about the best performing layout is mainly due to the different working conditions (i.e., heat source temperature, power size, operating pressures, assumed efficiencies etc.) at which these layouts are evaluated.

Consequently, a fair comparison can be hardly carried out. However, the reviewed literature highlights the high potential of the dual heated cascade which provides always a power output greater than or equal to that of the SS_DH layout. Thus, the thermal cuts of the single split double expansion basic configuration are solved by including two heaters (one for each stream: HE-1 and HE-2) and two regenerators (REG-1 and REG-2), in addition to the cooler (COOL), as shown in Fig. 4(a). According to Fig. 4(b), the splitter after the compressor generates the two streams 2' and 2''. The stream 2'' receives heat in two regeneration steps from different mass flow rates: in the second stage regenerator (REG-2) from the total mass flow rate (stream 8) and in the first stage regenerator (REG-1) from the mass flow rate of stream 2' (after the HTT expansion process, point 4). At the exit of REG-1 (point 6), the mass flow rate of stream 2" is further heated in the first stage heater (HE-1) and then expanded in the high temperature turbine (HTT). On the other side, the stream 2' goes through a second stage heater (HE-2) to be subsequently expanded in the low temperature turbine (LTT) and then re-injected between the two regenerators (at point 8).

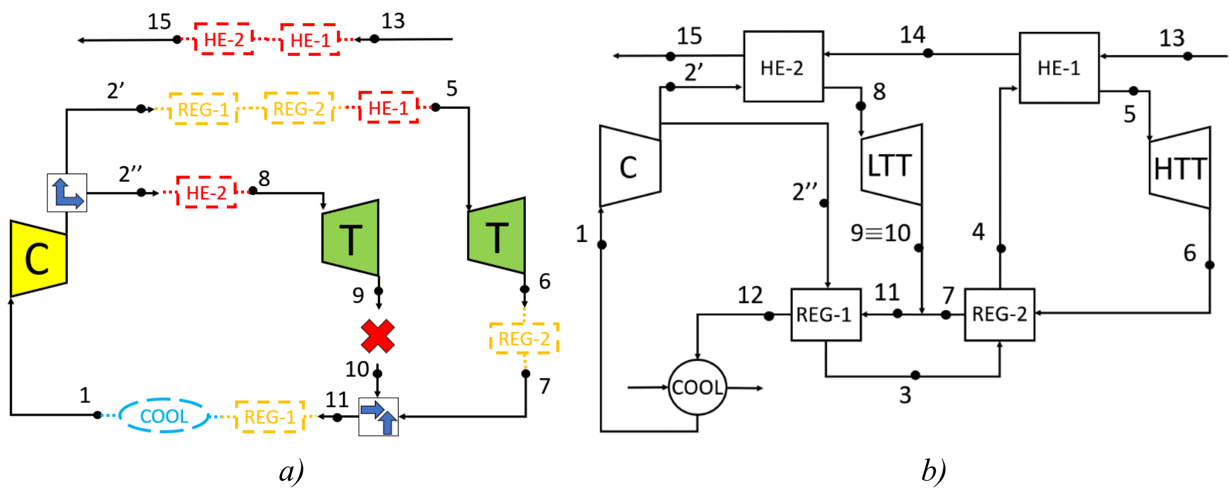

Fig. 4. Layout of the SS_DE configuration: a) integration of the heat exchanger network into the basic configuration of the Evolution Tree and b) the resulting configuration from a) proposed in the literature.

Taking as reference the work in [31], the main operating parameters of the SS_DE layout as bottoming cycle of a 5 MWe gas turbine are reported in Table 1.

3.4 Double split double heating

To the authors' knowledge, there are no configurations in the literature belonging to this cycle architecture. Thus, no layout is presented here. However, the DS_DH architecture in the form of Fig. 1 will be still optimized according to the HEATSEP method (Section 4.2). If better performances are obtained with respect to the other configurations, the heat exchanger network will be built and so a new configuration proposed. Fig. 5 shows the same "basic configuration" of the DS_DH layout in the Evolution Tree (Fig.1) with the addition of numbers at the extremities of the thermal cuts to enable a better comprehension of the composite curves presented in Section 5.

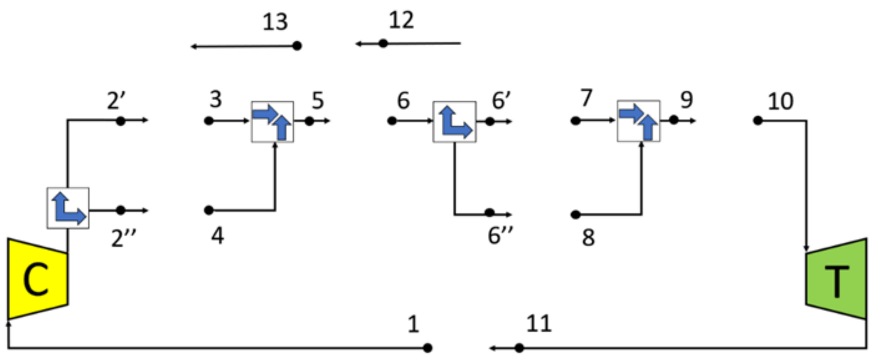

Fig. 5. Numbered basic configuration of the DS_DH layout.

3.5 Double split double expansion

Unlike the case of the SS_DE layout, more researchers [29, 31, 35] agree on the unbeatable performance of the dual flow split with dual expansion layout that matches with the double split double expansion (DS_DE) basic configuration (Fig. 1). The double split double expansion (DS_DE) configuration (Fig. 6) includes two splitters in the high pressure part of the cycle (Fig. 6(a)) to subdivide twice the mass flow rate after the compressor. This double splitting allows a higher flexibility in deciding the values of the mass flow rates through each heat exchanger. The aim is to further improve the thermal match in both heaters and regenerators, which leads to cool down as much as possible the heat source (i.e., maximize the heat recovery effectiveness) and to release as less heat as possible to the heat sink (i.e., maximize the thermal efficiency of the cycle). After the first splitter (Fig. 6(b)), a fraction of CO_2 (stream 2') is sent to a second stage heater (HE-2) while the rest (stream 2'') is sent to the second stage regenerator (REG-2), before they are mixed in 5. The re-joined stream is then split again into two different fractions, one (stream 6') to be expanded in a low temperature turbine (LTT) right after a first stage regenerator (REG-2) and the other one (stream 6'') to be heated in HE-1 before the inlet of the high temperature turbine (HTT). The CO_2 flow exiting the HTT is cooled in the REG-2 and then mixed with the CO_2 flow leaving the LTT. The overall CO_2 flow is cooled in the REG-1 (13–14) and finally in the cooler (14–1) to the desired compressor inlet temperature. Manente and Fortuna [29] thoroughly investigated the performance of the DS_DE layout for a wide range of heat source temperatures (400 °C – 800 °C). To be consistent with the working conditions shown in Table 1 for the other configurations, the operating parameters at the temperature of 500 °C are those selected from [29] and reported in Table 1.

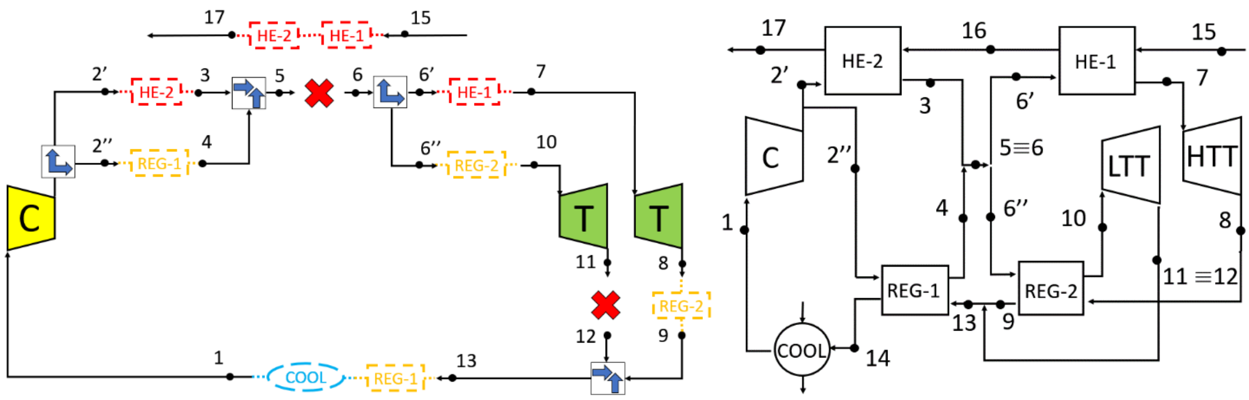

a) b)

Fig. 6. Layout of the DS_DE configuration: a) integration of the heat exchanger network into the basic configuration of the Evolution Tree and b) the resulting configuration from a) proposed in the literature.

Table 1. Operating parameters of the sCO₂ cycle configurations proposed in the literature derived from reference works.

Parameter	Value			
	Simple [47]	SS_DH [26]	SS_DE [31]	DS_DE [29]
$T_{in,hs}$ [°C]	470	538	519.7	500
$T_{out,hs}$ [°C]	212.6	73.8	87.7	95.7
$\dot{m}_{hs}$ [kg/s]	5.121	69.8	21.3	8.17
P [kW]	321.8	10640	3020	1000
TIT [°C]	363.1	398	440.9	450
p_{max} [bar]	201	230	273	200
p_{min} [bar]	76.3	57.3	88.7	76.3

4. Design optimization problem

This Section states the design optimization problem and describes the two different procedures used to optimize the *i)* configurations proposed in the literature on one side, and *ii)* the "basic configurations" evaluated with the HEATSEP method on the other side.

The design optimization problem of a cycle configuration is:

$$\text{find } \mathbf{x} \text{ which maximizes } P_{mec}(\mathbf{x}) \\ \text{subject to } \begin{cases} g(\mathbf{x}) = 0 \\ l(\mathbf{x}) > 0 \end{cases}, \tag{1}$$

where $\mathbf{x}$ is the array of the decision variables, $P_{mec}(\mathbf{x})$ is the objective function to be maximized (the mechanical power output), and $g(\mathbf{x})$ and $l(\mathbf{x})$ are the equations and inequalities of the design models of configuration components (see Appendix B).

The set of decision variables depends on the type of configurations to be optimized:

i) <u>Literature configurations</u>: the total CO_2 mass flow rate ($\dot{m}_{co2}$ [kg/s]]), the split flow ratio/s (i.e., the ratio between the fraction of the mass flow rate generated by a splitter and $\dot{m}_{co2}$) and the maximum cycle temperature (turbine inlet temperature (TIT) [°C]).

ii) <u>"Basic configurations" (from the Evolution Tree of Fig. 1)</u>: the total CO_2 mass flow rate ($\dot{m}_{co2}$ [kg/s]]), the split flow ratio/s (i.e., the ratio between the fraction of the mass flow rate generated by a splitter and $\dot{m}_{co2}$) and the downstream temperatures in each thermal cut (the upstream ones being fixed by preceding thermodynamic processes).

Table 2 shows the input parameters in the optimization and the temperature constraints imposed to the heat transfers between different fluids (i.e., CO_2/gas, CO_2/CO_2, CO_2/water).

The temperature and pressure at the inlet of the compressor and the pressure at the inlet of the turbine are set in accordance with various references found in the literature. Many authors suggest starting the compression process close to the critical point (76.3 bar, 32 °C) [31, 48] to minimize the compressor power consumption. On the other hand, the high inlet pressure limits the pressure ratio to values in the range 2.5-3 [49] in order to limit the maximum cycle pressure to approximately 200 bar. This value is a good compromise between technological issues and performance improvement deriving from higher pressures.

Table 2. sCO_2 Brayton-Joule cycles input parameters and heat transfer constraints.

Parameter	**Symbol**	**Value**
Heat source inlet temperature [°C]	$T_{hs,in}$	300, 500, 700
Compressor inlet pressure [bar]	$p_{in,c}$	76.3
Turbine inlet pressure [bar]	$p_{in,t}$	200
Compressor inlet temperature [°C]	T_1	32
Compressor isentropic efficiency [-]	$\eta_{is,c}$	0.66
Turbine isentropic efficiency [-]	$\eta_{is,t}$	0.81
Minimum temperature difference CO_2/gas [°C]	$\Delta T_{pp,CO_2/gas}$	35
Minimum temperature difference CO_2/ CO_2 [°C]	$\Delta T_{pp,CO_2/CO_2}$	15
Minimum temperature difference CO_2/water [°C]	$\Delta T_{pp,CO_2/water}$	5
Cooling water inlet temperature [°C]	$T_{w,in}$	27
Cooling water outlet temperature [°C]	$T_{w,out}$	40
Mechanical efficiency [-]	η_{mec}	0.98

Compressor and turbine isentropic efficiencies, minimum temperature difference in the flue gas heat exchanger, cooler, regenerator and the cooling water inlet/outlet temperatures are chosen according to manufacturers' data [47] (this choice is the simplest one to make an homogeneous comparison among different systems configurations, although the isentropic efficiencies vary depending on the boundary thermodynamic conditions). The cycle optimization is performed considering three different heat source temperatures (300 °C, 500 °C, 700 °C), which have been selected within an appropriate range of WHR applications [6]. For instance, 300 °C is the common temperature of flue gases deriving from the cement industry [50] while waste thermal streams between 500 °C and 700 °C are available from steel, iron and glass industry [47, 51, 52]. The flue gas is modeled as air having real gas properties.

4.1 Optimization of the configurations proposed in the literature

Engineering Equation Solver (EES®) software is used to implement the models of the configurations proposed in the literature (Appendix A). The optimization problem is solved using the conjugate directions method for multi-dimensional optimizations and the quadratic approximations method in case of a single decision variable. These two methods have been selected among those made available by the EES® optimization tool. The thermodynamic properties of carbon dioxide and of the gas mixture composing air (heat source) are provided by the internal library of EES® which uses the fundamental equations of state developed by Span and Wagner [53] and Lemmon et al. [54], respectively.

4.2 Optimization of the Evolution Tree configurations

The models of the "basic configurations" of the HEATSEP method (Evolution Tree in Fig. 1) are implemented in Matlab computer software (the models include the same equations implemented in EES, see Appendix A). The optimization problem is solved using the *fmincon* function which is a Nonlinear Programming solver provided by Matlab's Optimization Toolbox [55]. Note that *fmincon* minimizes the objective function that in this case becomes the opposite of the mechanical power output ($-P_{mec}(\mathbf{x})$). The configurations of the Evolution Tree are optimized without considering the presence of the heat exchangers as imposed by the HEATSEP method. However, the optimization method verifies at each iteration that the thermal streams allow building a feasible heat exchanger network (i.e., satisfying the pinch-point temperature constraints showed in Tab.1). Matlab retrieves the thermodynamic properties of carbon dioxide and air from the REFPROP database which implements the same equations of state used in EES® for CO_2 and air.

4.3 Performance Metrics

The performance parameters utilized in the present analysis are the thermal efficiency (η_{th} [-]), the maximum cycle temperature (TIT [°C]) and the mechanical power output (P_{mec}[kW]):

$$\eta_{th} = \frac{P_{mec}}{\dot{Q}_{av}} \tag{2}$$

$$P_{mec} = P_t - P_c - \frac{P_p}{\eta_{el}} - \frac{P_{cool}}{\eta_{el}} \tag{3}$$

$$\dot{Q}_{av} = \dot{m}_{gas} * (h_{in,gas} - h_{out,gas}) \tag{4}$$

where Q_{av}[kW] is the thermal power absorbed from the heat source, P_t [kW_m] is the turbine mechanical power, P_c[kW_m] the compressor mechanical power, η_{el}[-] the electrical efficiency of the generators, P_p[kW_e] and P_{cool}[kW_e] the electrical power of pumps and fans installed in the cooling towers, m_{gas}[kg/s] the gas mass flow rate and h[kJ/kg] represents enthalpy. The calculation of P_t, P_c, P_p, P_{cool} [kW] refers to the model of the configurations components, which are described in detail in Appendix B.

5. Results

In this Section, the results of the design optimization performed in EES (literature configurations) and using the HEATSEP method ("basic configurations" from the Evolution Tree in Fig.1) are compared and discussed. Table 3 summarizes the performance parameters (i.e., η_{th}, P_{mec} and TIT) of all the considered configurations for the three temperature levels of the heat source (Table 2). The optimized cycles of the literature configurations are shown in the T-s diagrams of Fig. 7, which follow the same enumeration of the figures in Section 3. On the other side, the composite curves resulting from the optimization of the "basic configurations" of the Evolution Tree are included in Fig. 8. All curves in Fig. 7 and in Fig. 8 refer to the intermediate heat source temperature of 500 °C, which is selected as the reference case. The composite curves related to the other two heat source temperatures (i.e., 300 and 700 °C) are included in Appendix C.

The T-s diagrams in Fig. 7 clearly highlight that the cycles featuring a double expansion (i.e., SS_DE and DS_DE) consist of a superimposition of two cycles. Between them, it is worth noticing the highest capability of the DS_DE layout (Fig. 7(d)) to increase the inlet temperatures of both turbines, achieving values of 465 °C and 345.4 °C for the low- and high-temperature turbines, respectively, in comparison with the values of 436.8 °C and 309.6 °C obtained with the SS_DE layout (Fig. 7(c)). Except for the “Simple” layout (Fig. 7(a)), all other configurations are able to cool down the heat source to the lowest temperature (according to the value of $\Delta T_{pp,CO_2/gas}$ in Table 2), confirming the potential of the strategy of splitting after the compressor to improve the heat recovery effectiveness.

In the following, the comparison between the results of the design optimization of the “literature” and “basic” configurations is carried out separately for each configuration. Conversely, the performances between the different configurations are compared in Section 5.1.

Simple regenerative (SIMPLE)

The power output obtained by the HEATSEP optimization is way higher than that resulting from the optimization of the literature configuration (444.7 kW vs 323 kW for the case of 500 °C). This outcome highlights the big room for improvement of the literature configuration that clearly does not accomplish an optimal heat transfer between the available heat fluxes.

However, the heat exchanger network of the SIMPLE configuration cannot satisfy the values of temperatures and mass flow rates given by the HEATSEP. To meet these requirements, the composite curves suggest that the two hot fluxes (i.e., CO_2 and the flue gas) should release heat to the cold one in the same temperature range (in between point 7 and 11 of Fig. 8(a)). Thus, it is necessary that each hot flux exchanges heat with a fraction of the cold one, thereby splitting its mass flow rate. The

HEATSEP solution suggests therefore to turn to more complex Evolution Tree configurations that include a split (see the next ones).

Single split double heating (SS_DH)

The SS_DH configuration in Fig. 3(b) is the best one attainable from the SS_DH basic configuration. In fact, the configuration proposed by the literature shows the same performance of the SS_DH basic configuration optimized with the HEATSEP method. It is worth pointing out that the composite curves of the SS_DH configuration (Fig. 8(a)) are the same of the SIMPLE one. Thus, the presence of a split and a junction at the same pressure level does not affect the capability of the HEATSEP method to optimize the thermal match between the cold and hot composite curves.

The thermal profiles of the curves at high temperature (between points 7-9 or 3-6 in Fig. 8(a)) show a diverging trend that indicates a non optimal thermal match and the presence of significant irreversibilities. This suggests that there are still chances for improvement from the thermodynamic point of view.

Single split double expansion (SS_DE)

The power output obtained by the optimization of the SS_DE configuration taken from the literature is very close to that achieved by the optimization of the “basic configuration” (e.g., 925 kW vs 925.8 kW for 700 °C, respectively). Thus, the optimal heat transfers suggested by the composite curves in Fig. 8(c) are effectively accomplished by the heat exchanger network of the SS_DE configuration in Fig. 4(b). The only exception is the thermal cut downstream of the low temperature turbine (red cross between points 9 and 10 in Fig. 4(a)). The composite curves of Fig. 8(c) show that the inclusion of this thermal cut allows increasing the turbines inlet temperature, resulting in a minor improvement of the performance of the “basic configuration” (478.1 kW vs 482.3 kW for the case of 500 °C, where this difference is more evident). The small contribution of the additional thermal cut is highlighted by the short line of the hot composite curve between points 9 and 10.

Table 3. Performance of the Literature and Evolution Tree configurations.

	η_{th} [%]			P_{mec} [kW]			TIT [°C]		
LITERATURE									
$\boldsymbol{T_{hs,in}}$ **[°C]**	***300***	***500***	***700***	***300***	***500***	***700***	***300***	***500***	***700***
Simple	14.4	21.0	27.0	114.6	323	578.8	265	373.5	500
SS_DH	14.8	20.5	26.0	131	444.7	864.0	265	354.4	464
SS_DE	14.4	22.1	27.9	114.6	478.1	925	265	436.8	550
DS_DH	-	-	-	-	-	-	-	-	-
DS_DE	14.8	23.2	28.7	131	502.5	953.6	265	465	665
EVOLUTION TREE									
Simple or SS_DH	14.9	20.5	25.8	131	444.7	860.4	265	353.9	460.5
SS_DE	12.3	22.2	27.8	131	482.3	925.8	265	465	550
DS_DH	14.9	20.5	25.7	131	445.1	856.3	265	354.2	457.9
DS_DE	11.6	23.2	28.7	131	502.5	953.9	265	465	665

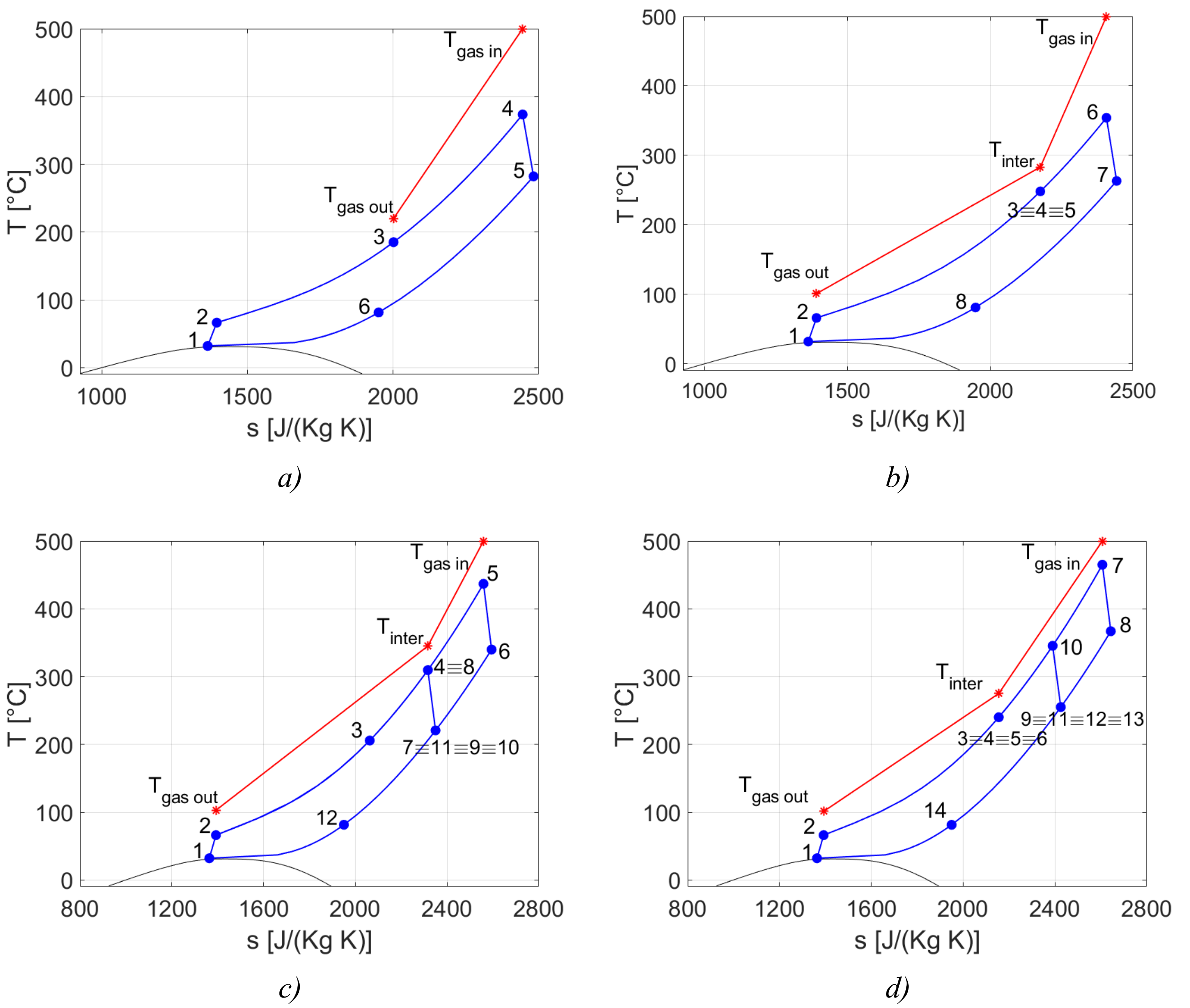

Fig. 7. T-s diagrams of the optimized literature configurations: a) SIMPLE; b) SS_DH; c) SS_DE; d) DS_DE.

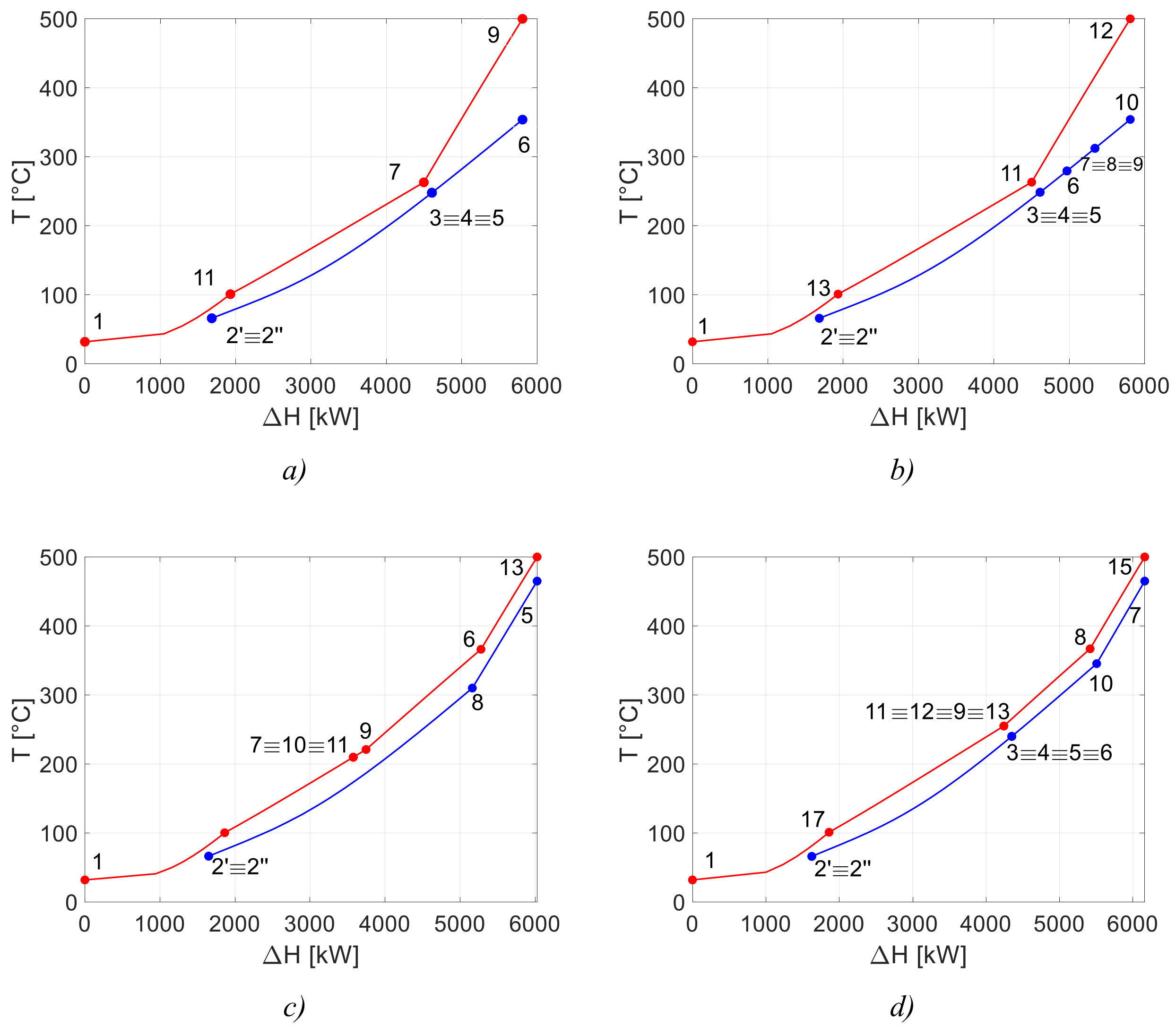

Fig. 8. Composite curves of the Evolution Tree configurations optimized with the HEATSEP *method: a) SIMPLE/SS_DH; b) DS_DH; c) SS_DE; d) DS_DE.*

These considerations confirm that the SS_DE configuration selected from the literature (i.e., the "dual heated cascade" layout, see Section 3) is able to achieve the highest power output among the other available candidates (i.e., the single flow split with dual expansion and the dual recuperated layouts). The power output of the SS_DE configuration could be increased of a few kilowatts only if a much more complex heat exchanger network is designed.

Finally, it is worth noticing that this "basic configuration" allows for a better thermal match in the high temperature range (between lines 13-6 of the hot curve and 8-5 of the cold one in Fig 8(c)) in comparison with the SS_DH basic configuration (between lines 9-7 of the hot curve and 9-3 of the cold one in Fig. 8(a)).

Double split double heating (DS_DH)

In spite of the increase of the available thermal cuts, the solution of the HEATSEP optimization does not differ from the one obtained from the SS_DH or the SIMPLE architectures. As a result, there is no need to proceed with the generation of the corresponding heat exchanger network, because it will certainly be more complex than the SS_DH one but not beneficial in terms of power production. As highlighted in the case of SS_DH, the HEATSEP method treats single or multiple splits and junctions at the same pressure level as points that are "free to move" along the same composite curve and do not constraint the optimization. This is clearly seen in Fig. 8(b) where the points 3-5 (junction 1), 6 (split 2) and 7-9 (junction 2) lay on a segment of the cold composite curve featuring a constant gradient.

Double split double expansion (DS_DE)

The very good agreement between the power outputs of the two optimization procedures (e.g., 502.5 kW vs 502.5 kW for 500 °C and 953.6 kW vs 953.9 kW for 700 °C) suggests that the DS_DE configuration proposed in the literature exploits optimally the thermal streams made available by the "basic configuration", being therefore the best candidate for the corresponding "basic configuration" in the Evolution Tree. It is important to highlight how the two additional thermal streams identified by the HEATSEP method in Fig. 6(a) (red crosses in between points 5-6 and 11-12) are not useful in the search for the best thermal match. In fact, Fig. 8(d) shows that the optimization of the "basic configuration" results in composite curves that do not include the heat transfers associated with these thermal streams (point 5 is superimposed on point 6 as well as point 11 is superimposed on point 12). The composite curves of this configuration show the best thermal match compared to the other configurations.

5.1 Comparison between the configurations

For medium-to-high temperatures of the heat source (i.e., 500 °C and 700 °C), the optimization of both literature and "basic configurations" shows an increase of power output that follows this order of configurations: SS_DH, SS_DE and DS_DE. By contrast, the optimization results obtained with a low temperature heat source (300 °C) indicate that i) the SS_DE and DS_DH literature configurations reduce to the SIMPLE and SS_DH ones, respectively, and that ii) all Evolution Tree configurations perform equally showing almost the same composite curves (see Appendix C). In general, all configurations show a power output ranging from 114.6 kW to 131 kW. Thus, for low temperature WHR applications the best configuration should be selected as the one that guarantees the best compromise between performance (power output) and economic feasibility (minimum number of components). According to this principle, the SS_DH literature configuration is the best one. Note that this configuration includes only one more component (additional heater) compared to the simplest one (SIMPLE).

6. Conclusions

A novel review approach is proposed in this paper to identify a common thread in the design of supercritical CO_2 power system configurations proposed in the scientific literature and specifically conceived for waste heat recovery applications. This approach is based on the HEATSEP method which indicates that the conceptual development of the system configurations relies on the evolution of "basic configurations" obtained by "cutting" all the thermal links between the ''basic'' components of the system, namely compressor, splitter, junction and turbine.

First, general rules can be derived by the critical review of the configurations available in the literature:

1. Supercritical CO_2 cycles can operate under limited pressure ratio because of the already high pressure at compressor inlet (close to the critical value, ~73 bar). This results in the need of

regeneration to achieve high power, and in turn limits the exploitation of heat source to the higher temperature range (i.e., to the range that is not covered by regeneration).

2. Characteristics and limits at point 1) suggest that high power output can be achieved only if the heating process is made independent of the regeneration one.
3. All the waste heat recovery-sCO_2 configurations in the literature contain at least one splitter after the compression to fulfill the requirement at point 2).
4. A novel perspective in the evolution of the waste heat recovery configurations is drawn depending on the location of the junction/s where the mass flow rates generated by the splitter/s re-join (heating or expansion zone).

Secondly, the optimization of the "basic configurations" (HEATSEP method) and of the corresponding configurations in the literature (including the heat exchanger network) allows for a comparative analysis. This comparison reveals that new and more performing configurations can be built by exploiting all the thermal interactions made available by the the HEATSEP method. However, if compared to existing literature configurations, these new layouts show slight improvements of the power output (the highest one is 4 kW out of 480 kW) that do not pay for the increased complexity and costs derived from the higher number of heat exchangers.

Further insights can be given by analysing more in detail the results of the comparative analysis:

- As regards configurations with one splitter-junction couple, the single split double expansion (SS_DE) layout outperforms the single split double heating (SS_DH) one for the heat source temperatures of 500 °C and 700 °C, improving the power output by 7.7 % and 7.1 %, respectively.
- The double split double expansion (DS_DE) configuration is the best performing one. Not only it achieves the highest power output but it also shows an almost perfect thermal match between the composite curves. Further changes to this configuration will be meaningless because they will unwisely complicate the layout without any important benefit.

- With an inlet temperature of the heat source equal to 300 °C, all basic configurations show the same performance, meaning that there is no need to complicate the layout with the addition of more thermal links. In particular, looking at the optimization results of the literature configurations, the best layout is the single split double heating (SS_DH) one because it achieves the highest power output and has the lowest number of components at the same time.
- The optimization based on the HEATSEP method (considering a temperature of the heat source equal to 500 °C) shows that the single split double expansion (SS_DE) basic configuration achieves a higher power output than the SS_DE literature configuration (482 kW vs 478 kW).

Finally, it is worth clarifying that the quite strict technological and economic boundary conditions of supercritical CO_2 systems may restrict the number of new design options and limit them to a set in which the higher complexity is not compensated by the additional costs. Thus, future research will necessarily consider techno-economic aspects in addition to the thermodynamic one. In particular, the framework of the sCO_2 layouts drawn in this work will be the basis for further investigating the most promising ones with a higher focus on the technological availability and cost of each component. This investigation will complete the current thermodynamic results, to give definitive guidelines for the choice of configurations that show high power output and are economically feasible at the same time.

Acknowledgements

This research did not receive any specific grant from funding agencies in the public, commercial, or not-for-profit sectors.

References

[1] Eurostat. Smarter, greener, more inclusive? Indicators to support the Europe 2020 strategy Publications Office of the European Union; 2019.

[2] Liao G, Liu L, E J, Zhang F, Chen J, Deng Y, et al. Effects of technical progress on performance and application of supercritical carbon dioxide power cycle: A review. Energy Conversion and Management. 2019;199:111986.

[3] Astolfi M, Alfani D, Lasala S, Macchi E. Comparison between ORC and CO2 power systems for the exploitation of low-medium temperature heat sources. Energy. 2018;161:1250-61.

[4] Kizilkan O. Performance assessment of steam Rankine cycle and sCO2 Brayton cycle for waste heat recovery in a cement plant: A comparative study for supercritical fluids. International Journal of Energy Research. 2020;44:12329-43.

[5] Persichilli M, Kacludis A, Zdankiewicz E, Held T. Supercritical CO2 power cycle developments and commercialization: why sCO2 can displace steam ste. Power-Gen India & Central Asia. 2012;2012:19-21.

[6] White MT, Bianchi G, Chai L, Tassou SA, Sayma AI. Review of supercritical CO2 technologies and systems for power generation. Applied Thermal Engineering. 2021;185:116447.

[7] Dostal V, Driscoll MJ, Hejzlar P. A supercritical carbon dioxide cycle for next generation nuclear reactors: Massachusetts Institute of Technology, Department of Nuclear Engineering; 2004.

[8] Park JH, Park HS, Kwon JG, Kim TH, Kim MH. Optimization and thermodynamic analysis of supercritical CO2 Brayton recompression cycle for various small modular reactors. Energy. 2018;160:520-35.

[9] Turchi CS, Ma Z, Neises TW, Wagner MJ. Thermodynamic Study of Advanced Supercritical Carbon Dioxide Power Cycles for Concentrating Solar Power Systems. Journal of Solar Energy Engineering. 2013;135.

[10] Ahn Y, Bae SJ, Kim M, Cho SK, Baik S, Lee JI, et al. Review of supercritical CO2 power cycle technology and current status of research and development. Nuclear Engineering and Technology. 2015;47:647-61.

[11] Reyes-Belmonte MA, Sebastián A, Romero M, González-Aguilar J. Optimization of a recompression supercritical carbon dioxide cycle for an innovative central receiver solar power plant. Energy. 2016;112:17-27.

[12] Anderson RE, MacAdam S, Viteri F, Davies DO, Downs JP, Paliszewski A. Adapting Gas Turbines to Zero Emission Oxy-Fuel Power Plants. ASME Turbo Expo 2008: Power for Land, Sea, and Air2008. p. 781-91.

[13] Sanz W, Jericha H, Moser M, Heitmeir F. Thermodynamic and Economic Investigation of an Improved Graz Cycle Power Plant for CO2 Capture. Journal of Engineering for Gas Turbines and Power. 2005;127:765-72.

[14] Costamagna P. Three-pipeline gas grid: A new concept for power-to-gas associated with complete carbon capture and utilization. Energy Conversion and Management. 2021;229:113739.

[15] Carraro G, Manente G, Lazzaretto A. Review of the best technologies for the exploitation of low-to-medium temperature heat sources: From ORC to sCO2 power cycles. ECOS 2018 - Proceedings of the 31st International Conference on Efficiency, Cost, Optimization, Simulation and Environmental Impact of Energy Systems2018.

[16] Sharma OP, Kaushik SC, Manjunath K. Thermodynamic analysis and optimization of a supercritical CO2 regenerative recompression Brayton cycle coupled with a marine gas turbine for shipboard waste heat recovery. Thermal Science and Engineering Progress. 2017;3:62-74.

[17] Mohammadi K, McGowan JG. Thermoeconomic analysis of multi-stage recuperative Brayton cycles: Part II – Waste energy recovery using CO2 and organic Rankine power cycles. Energy Conversion and Management. 2019;185:920-34.

[18] Moroz L, Burlaka M, Rudenko O, Joly C. Evaluation of gas turbine exhaust heat recovery utilizing composite supercritical CO2 cycle. Proceedings of the International Gas Turbine Congress, Tokyo, Japan2015. p. 15-20.

[19] Binotti M, Astolfi M, Campanari S, Manzolini G, Silva P. Preliminary assessment of sCO2 cycles for power generation in CSP solar tower plants. Applied Energy. 2017;204:1007-17.

[20] Manente G, Lazzaretto A. Innovative biomass to power conversion systems based on cascaded supercritical CO2 Brayton cycles. Biomass and Bioenergy. 2014;69:155-68.

[21] Hou S, Wu Y, Zhou Y, Yu L. Performance analysis of the combined supercritical CO2 recompression and regenerative cycle used in waste heat recovery of marine gas turbine. Energy Conversion and Management. 2017;151:73-85.

[22] Hou S, Zhou Y, Yu L, Zhang F, Cao S. Optimization of the combined supercritical CO2 cycle and organic Rankine cycle using zeotropic mixtures for gas turbine waste heat recovery. Energy Conversion and Management. 2018;160:313-25.

[23] Liu Y, Wang Y, Huang D. Supercritical CO2 Brayton cycle: A state-of-the-art review. Energy. 2019;189:115900.

[24] Crespi F, Gavagnin G, Sánchez D, Martínez GS. Supercritical carbon dioxide cycles for power generation: A review. Applied Energy. 2017;195:152-83.

[25] Sánchez Villafana ED, Vargas Machuca Bueno JP. Thermoeconomic and environmental analysis and optimization of the supercritical CO2 cycle integration in a simple cycle power plant. Applied Thermal Engineering. 2019;152:1-12.

[26] Kim YM, Sohn JL, Yoon ES. Supercritical CO2 Rankine cycles for waste heat recovery from gas turbine. Energy. 2017;118:893-905.

[27] Na S-I, Kim MS, Baik Y-J, Kim M. Optimal allocation of heat exchangers in a Supercritical carbon dioxide power cycle for waste heat recovery. Energy Conversion and Management. 2019;199:112002.

[28] Song J, Ren X-d, Gu C-w. Investigation of Engine Waste Heat Recovery Using Supercritical CO2(S-CO2) Cycle System. ASME Turbo Expo 2018: Turbomachinery Technical Conference and Exposition2018.

[29] Manente G, Fortuna FM. Supercritical CO2 power cycles for waste heat recovery: A systematic comparison between traditional and novel layouts with dual expansion. Energy Conversion and Management. 2019;197:111777.

[30] Wright SA, Davidson CS, Scammell WO. Thermo-economic analysis of four sCO2 waste heat recovery power systems. Fifth International SCO2 Symposium, San Antonio, TX, Mar2016. p. 28-31.

[31] Kim MS, Ahn Y, Kim B, Lee JI. Study on the supercritical CO2 power cycles for landfill gas firing gas turbine bottoming cycle. Energy. 2016;111:893-909.

[32] Manente G, Costa M. On the Conceptual Design of Novel Supercritical CO2 Power Cycles for Waste Heat Recovery. Energies. 2020;13:370.

[33] Morandin M, Toffolo A, Lazzaretto A. Superimposition of Elementary Thermodynamic Cycles and Separation of the Heat Transfer Section in Energy Systems Analysis. Journal of Energy Resources Technology. 2013;135.

[34] Marchionni M, Bianchi G, Tassou SA. Techno-economic assessment of Joule-Brayton cycle architectures for heat to power conversion from high-grade heat sources using CO2 in the supercritical state. Energy. 2018;148:1140-52.

[35] Kimzey G. Development of a Brayton bottoming cycle using supercritical carbon dioxide as the working fluid. Electric Power Research Institute, University Turbine Systems Research Program, Gas Turbine Industrial Fellowship, Palo Alto, CA. 2012.

[36] Thanganadar D, Asfand F, Patchigolla K. Thermal performance and economic analysis of supercritical Carbon Dioxide cycles in combined cycle power plant. Applied Energy. 2019;255:113836.

[37] Held TJ. Supercritical CO2 cycles for gas turbine combined cycle power plants. Power Gen Int. 2015.

[38] Lazzaretto A, Toffolo A. A method to separate the problem of heat transfer interactions in the synthesis of thermal systems. Energy. 2008;33:163-70.

[39] Toffolo A, Lazzaretto A, Morandin M. The HEATSEP method for the synthesis of thermal systems: An application to the S-Graz cycle. Energy. 2010;35:976-81.

[40] Held TJ. Initial test results of a megawatt-class supercritical CO2 heat engine. The 4th International Symposium–Supercritical CO2 Power Cycles2014. p. 9-10.

[41] Huang G, Shu G, Tian H, Shi L, Zhuge W, Zhang J, et al. Development and experimental study of a supercritical CO2 axial turbine applied for engine waste heat recovery. Applied Energy. 2020;257:113997.

[42] Moore J, Brun K, Evans N, Kalra C. Development of 1 MWe Supercritical CO2 Test Loop. ASME Turbo Expo 2015: Turbine Technical Conference and Exposition2015.

[43] Lazzaretto A, Segato F. Thermodynamic Optimization of the HAT Cycle Plant Structure—Part I: Optimization of the "Basic Plant Configuration". Journal of Engineering for Gas Turbines and Power. 2000;123:1-7.

[44] Lazzaretto A, Segato F. Thermodynamic Optimization of the HAT Cycle Plant Structure—Part II: Structure of the Heat Exchanger Network. Journal of Engineering for Gas Turbines and Power. 2000;123:8-16.

[45] Mohagheghi M, Kapat J. Thermodynamic optimization of recuperated S-CO2 Brayton cycles for waste heat recovery applications. 4th International Supercritical CO2 Power Cycles Symposium: Citeseer; 2014.

[46] Wang K, Li M-J, Guo J-Q, Li P, Liu Z-B. A systematic comparison of different S-CO2 Brayton cycle layouts based on multi-objective optimization for applications in solar power tower plants. Applied Energy. 2018;212:109-21.

[47] Danieli P, Rech S, Lazzaretto A. Supercritical CO2 and air Brayton-Joule versus ORC systems for heat recovery from glass furnaces: Performance and economic evaluation. Energy. 2019;168:295-309.

[48] Liu M, Zhang X, Yang K, Ma Y, Yan J. Optimization and comparison on supercritical CO2 power cycles integrated within coal-fired power plants considering the hot and cold end characteristics. Energy Conversion and Management. 2019;195:854-65.

[49] Edited by Klaus Brun PF, Richard Dennis. Fundamentals and Applications of Supercritical Carbon Dioxide (SCO2) Based Power Cycles. 1st ed: Woodhead Publishing; 2017.

[50] Karellas S, Leontaritis AD, Panousis G, Bellos E, Kakaras E. Energetic and exergetic analysis of waste heat recovery systems in the cement industry. Energy. 2013;58:147-56.

[51] Zhang L. Waste Heat Recovery from Metal Industries. JOM. 2012;64:982-4.

[52] Korobitsyn M. Industrial applications of the air bottoming cycle. Energy Conversion and Management. 2002;43:1311-22.

[53] Span R, Wagner W. A New Equation of State for Carbon Dioxide Covering the Fluid Region from the Triple-Point Temperature to 1100 K at Pressures up to 800 MPa. Journal of Physical and Chemical Reference Data. 1996;25:1509-96.

[54] Lemmon EW, Jacobsen RT, Penoncello SG, Friend DG. Thermodynamic Properties of Air and Mixtures of Nitrogen, Argon, and Oxygen From 60 to 2000 K at Pressures to 2000 MPa. Journal of Physical and Chemical Reference Data. 2000;29:331-85.

[55] fmincon. Matlab 2019b, The Mathworks Inc, Natick, Massachusetts, USA. https://it.mathworks.com/help/optim/ug/fmincon.html.

[56] Song J, Li X-s, Ren X-d, Gu C-w. Performance improvement of a preheating supercritical CO2 (S-CO2) cycle based system for engine waste heat recovery. Energy Conversion and Management. 2018;161:225-33.

[57] Wang S-s, Wu C, Li J. Exergoeconomic analysis and optimization of single-pressure single-stage and multi-stage CO2 transcritical power cycles for engine waste heat recovery: A comparative study. Energy. 2018;142:559-77.

APPENDIX A

Table A.1 lists the characteristics of the main sCO_2 configurations for waste heat recovery available in the literature. Particularly, for each configuration, it specifies the name, shows a schematic of the layout and presents the performance obtained by three reference works from the literature.

Table A.1. Summary of the most used WHR sCO_2 configurations with performance data from the literature

#	Name	Layout	T_{hs} [°C]	P_{el} [kW]	η_{th} [%]	Ref.	Legend
a)	Simple regenerative	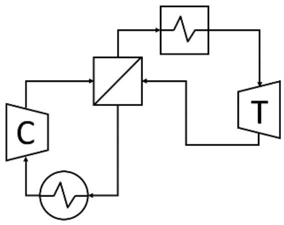	470	321.8	20.4	[47]	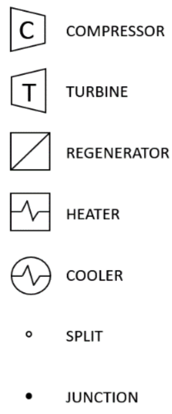
			396	1459	25.9	[17]	
			450	9500	30*	[3]	
b)	Recompression	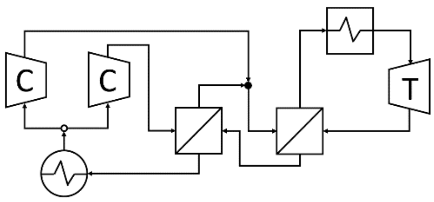	550	11300	20.5*	[18]	
			572	3842	32.2	[16]	
			530	10000	/	[45]	
c)	Partial heating	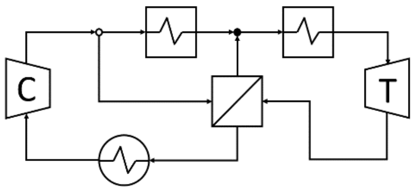	532	8600	18	[27]	
			538	10640	29	[26]	
			300	68.4	/	[56]	
d)	Single flow split with dual expansion	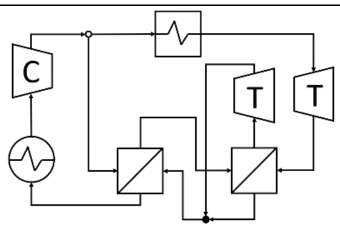	520	2680	27.6	[31]	
			600	1000	26.6	[32]	
			538	8214	26.5	[30]	
e)	Dual recuperated	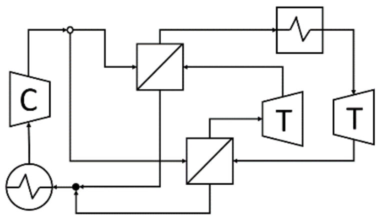	470	484	28.4	[57]	
			538	8322	28.2	[30]	
			600	1000	28.4	[32]	
f)	Dual heated cascade	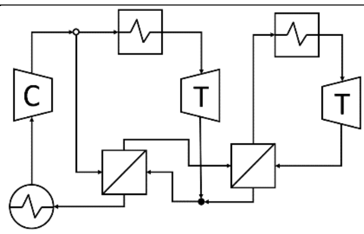	520	3020	30.2	[31]	
			471, 625	13400, 145000	24.8, 31.2	[35]	
			650	160	26	[34]	
g)	Dual flow split with dual expansion	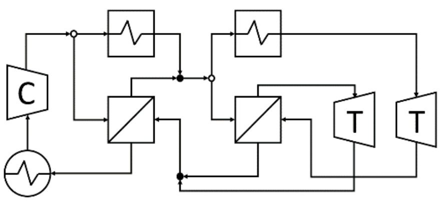	520	3230	31.7	[31]	
			400-800	1000	22.2-31.6	[29]	
			471, 625	15200, 169000	27, 35.2	[35]	

*Total efficiency (η_{tot})

APPENDIX B

B.1 Models of the components

Turbomachinery
The mass and energy balance equations of pumps, compressors and turbines are

$$\dot{m}_{in} = \dot{m}_{out} = \dot{m}, \tag{B.1}$$

$$P_{mec} = \dot{m} \cdot |h_{in} - h_{out}| \cdot \eta_m, \tag{B.2}$$

where η_{mec} is the mechanical efficiency, and h_{in} and h_{out} are the enthalpies at component inlet and outlet, respectively. Outlet enthalpies are calculated as follows

$$\text{Compressors/pumps:} \quad h_{out} = h_{in} + \frac{h_{out,is} - h_{in}}{\eta_{is}} \tag{B.3}$$

$$\text{Turbines:} \quad h_{out} = h_{in} - \eta_{is} \cdot (h_{in} - h_{out,is}) \tag{B.4}$$

where η_{is} is the isentropic efficiency of the component and $h_{out,is}$ is the enthalpy at the component outlet in the reference isentropic process, which is calculated starting from the inlet pressure and temperature (p_{in} and T_{in}), and outlet pressure (p_{out}). So, the temperature at the component outlet (T_{out}) can be obtained from h_{out} and p_{out}.

Heat exchangers
The model of the heat exchangers is simply made up of mass and energy balances:

$$\dot{m}_{1,in} = \dot{m}_{1,out} \quad \text{and} \quad \dot{m}_{2,in} = \dot{m}_{2,out} \tag{B.5}$$

$$\dot{m}_{1,in} \cdot \left(h_{1,in} - h_{1,out}\right) = \dot{m}_{2,in} \cdot \left(h_{2,out} - h_{2,in}\right) = \dot{Q} \tag{B.6}$$

where the subscripts 1 and 2 refer to the hot and cold side of the heat exchanger, respectively.

Cooling towers
The power consumption of the fans of the cooling tower are calculated by the following equation, which was obtained by interpolating data from several cooling towers manufacturers [47]

$$P_{cool} = 0.0123 * Q_{cool} - 0.7622. \tag{B.7}$$

APPENDIX C

Figures C.1 and C.2 show the composite curves in the cases of heat source temperatures of 300 °C and 700 °C, respectively.

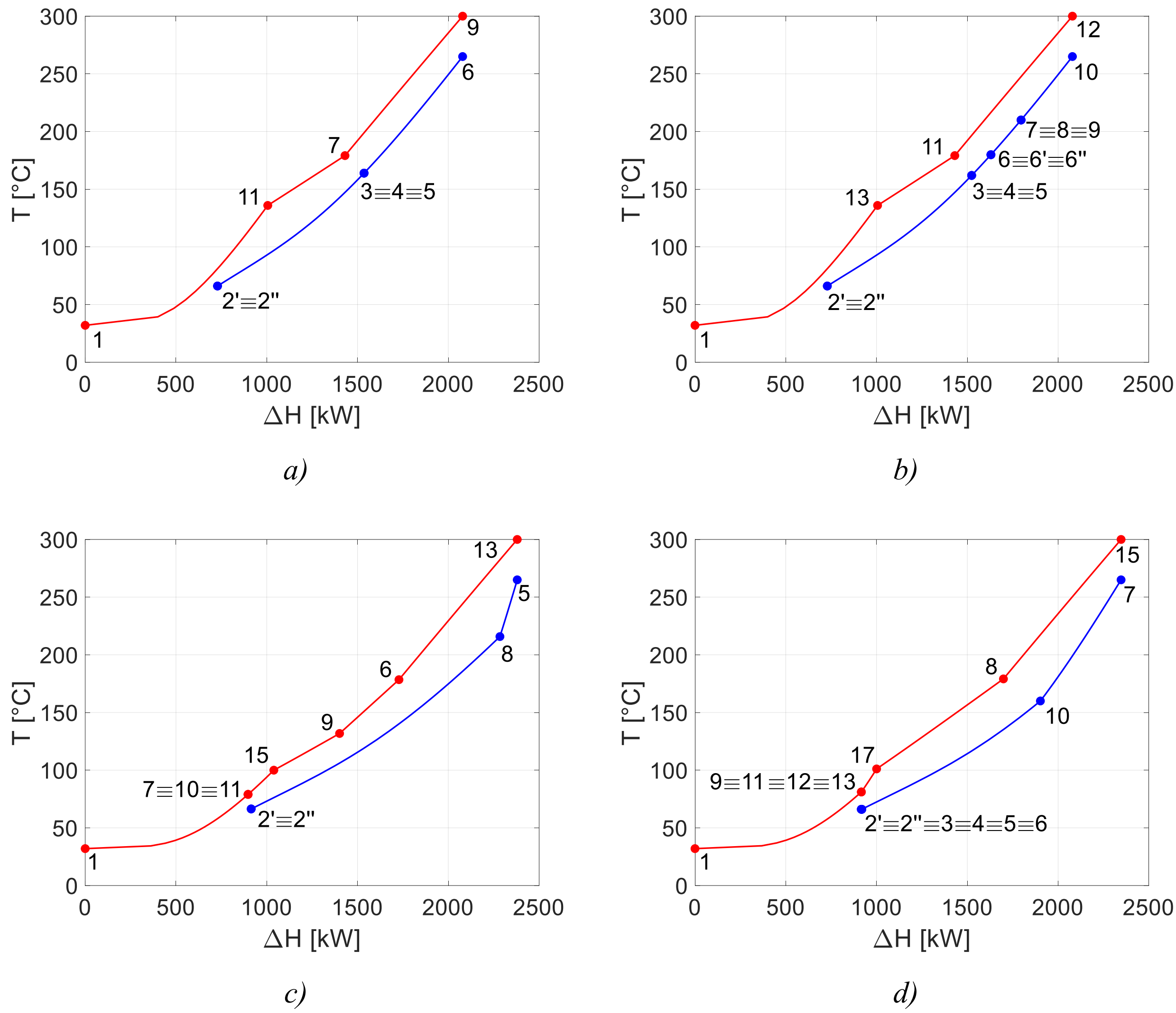

Fig. C.1. Composite curves of the basic configurations optimized with the HEATSEP *method (heat source temperature of 300 °C): a) SIMPLE/SS_DH; b) DS_DH; c) SS_DE; d) DS_DE.*

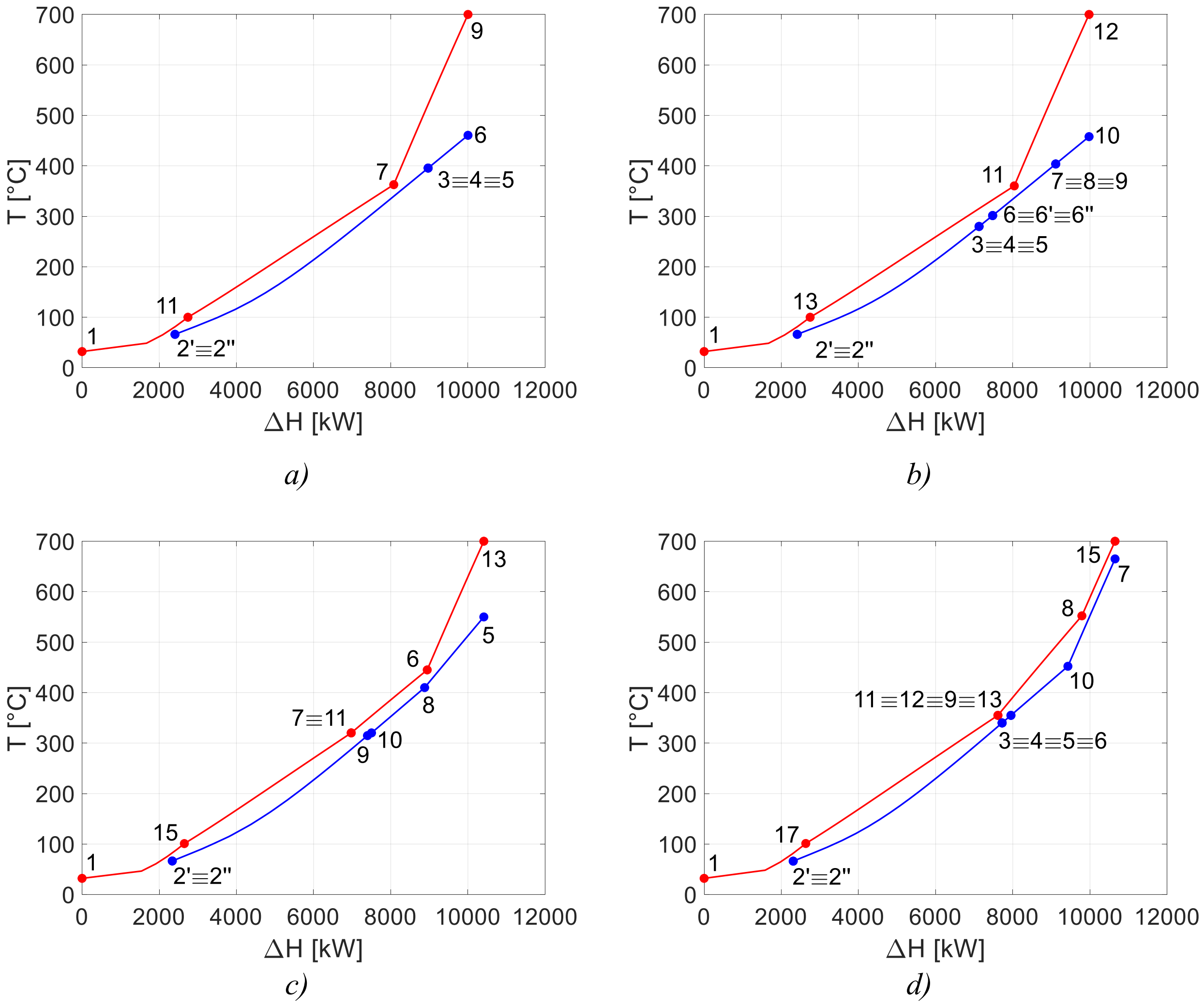

Fig. C.2. Composite curves of the basic configurations optimized with the HEATSEP *method (heat source temperature of 700 °C): a) SIMPLE/SS_DH; b) DS_DH; c) SS_DE; d) DS_DE.*